Phonon-Induced Gaps in Graphene and Graphite Observed by Angle-Resolved Photoemission

Y. Liu, Longxiang Zhang, M. K. Brinkley, G. Bian, T. Miller, and T.-C. Chiang*

Department of Physics, University of Illinois at Urbana-Champaign, 1110 West Green Street, Urbana, Illinois 61801-3080, USA, and Frederick Seitz Materials Research Laboratory, University of Illinois at Urbana-Champaign, 104 South Goodwin Avenue, Urbana, Illinois 61801-2902, USA

(Received 2 June 2010; published 23 September 2010)

Mapping by angle-resolved photoemission spectroscopy of the spectral functions of graphite and graphene layers at low temperatures reveals a heretofore unreported gap of ~67 meV at normal emission. This gap persists to room temperature and beyond, and diminishes for increasing emission angles. We show that this gap arises from electronic coupling to out-of-plane vibrational modes at the $\bar{K}$ point in the surface Brillouin zone in accordance with conservation laws and selection rules governed by quantum mechanics. Our study suggests a new approach for characterizing phonons and electron-phonon coupling in solids.

DOI: 10.1103/PhysRevLett.105.136804 PACS numbers: 73.22.Pr, 71.38.−k, 79.60.Jv

Angle-resolved photoemission spectroscopy (ARPES) is a powerful technique for determining the electronic structure of materials, and it has been applied to numerous systems of scientific and technological interest [1]. The measured spectral functions are related to the quasiparticle self-energies, which are influenced by interactions with elementary excitations including phonons. Electron-phonon coupling is of special interest as it plays a key role in the formation of charge density waves and superconducting states. Its main signature is the ''kinks'' in dispersion relations near the Fermi level, which have been well documented for a variety of systems including graphene layers of various thicknesses and configurations [2–6]. While strong interest in the electronic structure of these graphitic materials has driven extensive ARPES studies [2,3,7–10], prior work has mostly focused on the quasiparticle band dispersion relations associated with the Dirac cones. Largely unexplored are spectral regions far away from the quasiparticle bands, where direct emission from the quasiparticles is forbidden, but indirect emission through coupling to phonons is allowed. Our work shows that ARPES measurements within the forbidden region can yield valuable information about high-order processes such as electron-phonon coupling. Specifically, the experiment reveals a gap of ~67 meV at low temperatures for several graphitic materials including highly oriented pyrolitic graphite (HOPG), natural single-crystal graphite (NSCG), and few-layer graphene (FLG) systems prepared on SiC(0001). A detailed study of the temperature and angular dependences of the gap suggests that the gap arises from out-of-plane vibrational modes at the $\bar{K}$ point, which dominate the coupling to electrons at normal emission.

Our ARPES measurements were performed at the Synchrotron Radiation Center, University of Wisconsin-Madison, using the PGM-A, U-NIM, and Wadsworth beam lines. The energy and momentum resolutions were 20 meV and 0.01 Å^{-1}, respectively. All spectra were taken with the sample temperature at 60 K, unless otherwise stated. The results from these three samples are similar; this is not surprising since graphite is essentially a stack of graphene layers weakly bonded together by van der Waals forces.

Figure 1 shows the electronic band structures and phonon dispersion relations for graphite and graphene obtained from first-principles calculations based on the ABINIT program [11–14]. These calculations based on the LDA approximation yield a fairly good overall description of the experiment; more accurate results based on the *GW* approximation are available in the literature [15,16]. The calculated results are very similar for graphene and graphite within the basal plane. The dispersions for graphite are small along the z direction (perpendicular to

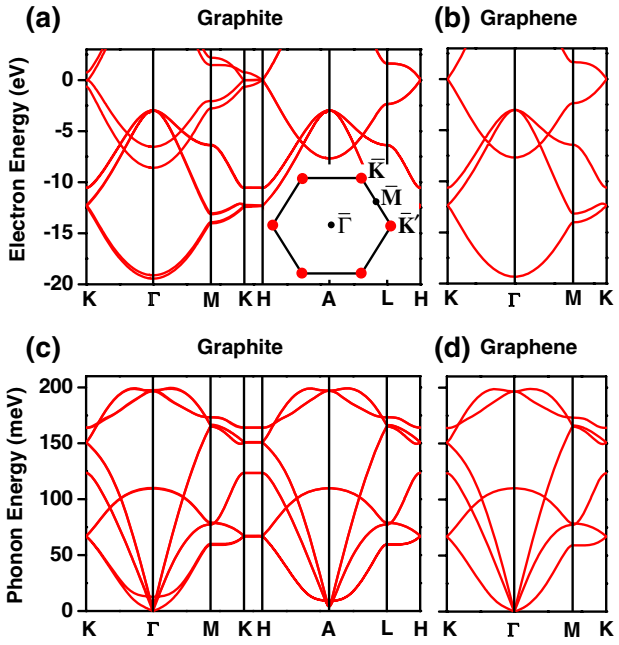

FIG. 1 (color online). Band structures and phonon dispersion relations of graphite (a), (c) and graphene (b), (d) from first-principles calculations. The inset in (a) shows schematically the two-dimensional Fermi surface of graphite and graphene, which consists of 6 Dirac points at $\bar{K}$ and $\bar{K}'$.

the basal plane). Of special interest are the phonons at the K point of graphene and along K-H in graphite. Their energies are essentially identical. For simplicity, the discussion below will mostly refer to the graphene dispersion relations. Generalization to graphite is straightforward.

The ARPES spectrum at normal emission from HOPG at 60 K [Fig. 2(a)] shows a peak derived from the π band at about -8.5 eV. Emission at angles near the K point [Fig. 2(b)] shows a quasi-Dirac cone from the π band. The random in-plane orientation of graphite crystallites in HOPG dilutes the emission intensity from the Dirac cone, making this feature very weak. Detailed spectra at normal emission and near K [Fig. 2(c)] reveal a gap near the Fermi level at normal emission, as evidenced by a comparison to the spectrum from a reference Ag film. The spectrum at normal emission is very weak as indicated by the relative scales. It actually contains a tiny Fermi edge, which is likely caused by defects [17]. The inset shows the spectrum at normal emission symmetrized about the Fermi level (see supplementary document [18]), which clearly shows a gap of about ± 67 meV in an approximately linear spectrum. This gap, independent of the photon energy, becomes less distinct at higher temperatures [Fig. 2(d)] but remains visible at room temperature. Similar results are obtained from a NSCG [Fig. 2(e)], but there is a somewhat higher background in the gap likely caused by impurities and defects in natural crystals.

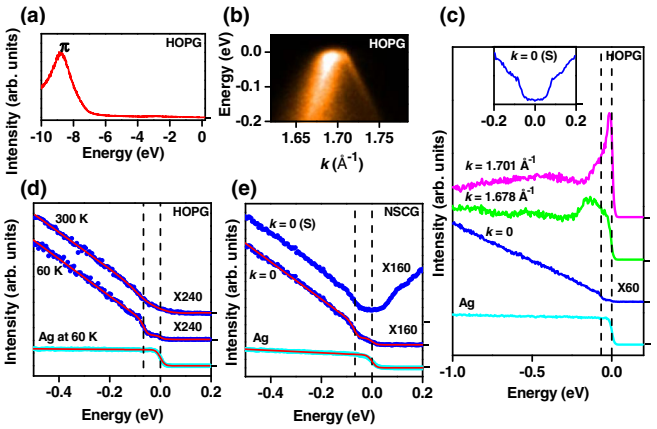

FIG. 2 (color online). ARPES results from HOPG [(a), (b), (c), (d)] and NSCG (e). (a) Normal emission spectrum of HOPG. (b) Measured dispersion of HOPG near $\bar{K}$ along a radial direction pointed away from $\bar{\Gamma}$. (c) Spectra at various in-plane momenta $\mathbf{k}$ for HOPG and a reference spectrum from Ag. The inset is a zoom-in view of the gap near the Fermi level, obtained by symmetrizing (labeled S) the normal emission spectrum with respect to the Fermi level. (d), (e) Comparison between fits (red [medium gray] curves) and normal emission spectra for HOPG (d) and NSCG (e). The vertical dash lines indicate positions of the Fermi level and the edge of the gap. The zero level for each spectrum is indicated by a tick mark on the right vertical axis. The photon energy used was 22 eV. The sample was at 60 K in all cases except for those labeled otherwise.

A similar gap is also observed in FLG. The number of monolayers (MLs) of graphene can be deduced from the Dirac-cone feature near the K point [Fig. 3(a)] [8,9]. Emission from the Si $2p$ core level [Fig. 3(b)] decays rapidly for increasing graphene coverages because of a short photoelectron escape depth [19]. At normal emission, the $6\sqrt{3} \times 6\sqrt{3}$ surface exhibits a broad surface state at about -0.6 eV [Fig. 3(c)] [20]. It becomes an interface state under graphene coverage, and its intensity is attenuated rapidly with increasing graphene coverages. At small graphene coverages, the long tail of the interface state enters into the gap region and interferes with line shape analysis. As a result, the gap is not obvious at 1 ML, but it is quite clear for the thicker graphene layers (2–4 MLs). In each case, there is a metallic Fermi edge, likely due to defects. The gap is clearly seen in the enlarged views of the 3 and 4 ML data and their symmetrized versions [Fig. 3(d)]. Also included is a spectrum for the 3 ML sample near the K point, which shows no gap. The gap feature for the 4 ML case is somewhat weaker, possibly

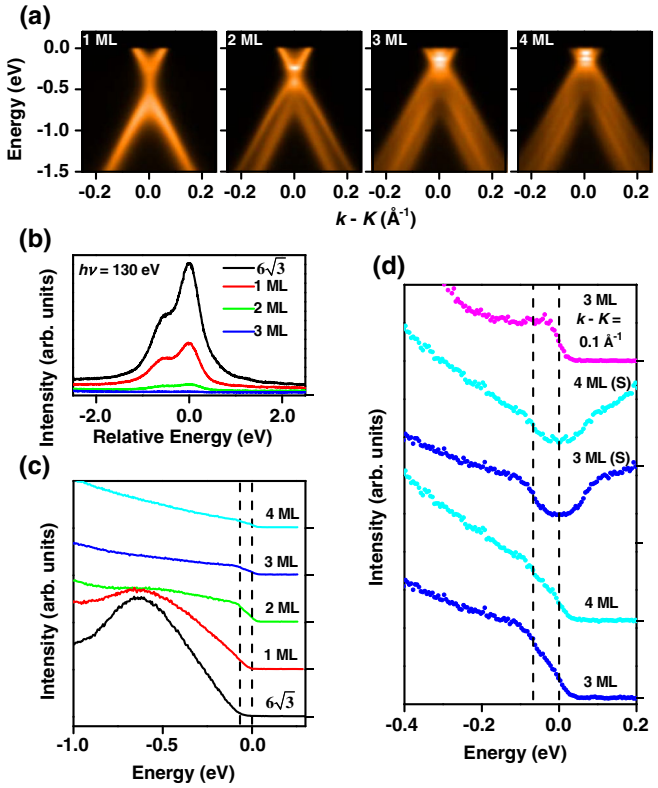

FIG. 3 (color online). ARPES result from FLG on 6H-SiC. (a) Evolution of the Dirac-cone features near the $\bar{K}$ point measured along a direction perpendicular to $\bar{\Gamma}\,\bar{K}$. (b) Si $2p$ core level. (c) Normal emission spectra as a function of graphene layer thickness. (d) Normal emission spectra and symmetrized versions (labeled S) near the Fermi level for 3 and 4 ML graphene layers. Also shown for comparison is a spectrum near the K point. The zero level for each spectrum is indicated by a tick mark on the right vertical axis. The photon energy used was 50 eV in all cases, except (b) for which 130 eV photons were used.

caused by increased roughness at higher graphene coverages (see [18]) [7].

Because of the large band gap around the Fermi level at the zone center (Fig. 1), the observed gap feature must involve higher order processes. The only states nearby in energy are near the K point. Momentum conservation for normal emission from these states requires the involvement of either an elementary excitation near the K point or a defect. Defect scattering, being strictly energy conserving, cannot account for the gap. Phonon scattering is the only plausible explanation.

The initial state at the K point for graphene is

$$\psi_{\mathbf{K}}(\mathbf{r}) \propto \sum_{\mathbf{R}} \phi(\mathbf{r}-\mathbf{R}) \exp(i\mathbf{K}\cdot\mathbf{R}), \tag{1}$$

where $\phi(\mathbf{r})$ is a carbon p_z orbital, $\mathbf{K}$ is the wave vector at the K point, and the summation is over all lattice vectors $\mathbf{R}$. The orbital $\phi(\mathbf{r})$ is of even parity within the basal plane. There are actually two degenerate states; the other one involves a p_z orbital centered about the other atom within the unit cell. Photoexcitation of $\psi_{\mathbf{K}}(\mathbf{r})$ leads to

$$\psi'_{\mathbf{K}}(\mathbf{r}) \propto \sum_{\mathbf{R}} \phi'(\mathbf{r}-\mathbf{R}) \exp(i\mathbf{K}\cdot\mathbf{R}), \tag{2}$$

where ϕ' is an excited Wannier function. The excitation involves the usual dipole transition term and a ''surface transition'' term arising from a nonzero $\nabla\cdot\mathbf{A}$, where $\mathbf{A}$ is the vector potential [21,22]. Both terms are important for three-dimensional systems, but only the dipole term preserves the crystal momentum along z. Graphite is a quasi-two-dimensional crystal with a large perpendicular lattice constant $c = 6.7$ Å compared to the z extent of the p_z orbital of about $a = 1.4$ Å; the dipole term is scaled down by a factor of $\sim(a/c)^2$. As a result, surface transitions dominate. Since this involves a z-dependent interaction, the in-plane parity of the state is preserved. Thus, ϕ' is also of even parity within the basal plane.

The state $\psi'_{\mathbf{K}}$ can couple via a phonon of wave vector $-\mathbf{K}$ to a state at the zone center:

$$\psi''_0(\mathbf{r}) \propto \sum_{\mathbf{R}} \phi''(\mathbf{r}-\mathbf{R}), \tag{3}$$

where ϕ'' is another excited Wannier function. This state can couple to a plane wave in vacuum, leading to normal emission, if ϕ'' is of even parity within the basal plane [23]. Within the usual rigid-ion approximation, the electron-phonon coupling is

$$\Delta H \propto Q\langle\phi''(\mathbf{r})|\mathbf{e}\cdot\nabla V(\mathbf{r})|\phi'(\mathbf{r})\rangle, \tag{4}$$

where V is the ionic potential, $\mathbf{e}$ is the phonon polarization vector, and Q is the phonon normal mode coordinate. Because both ϕ' and ϕ'' are of even parity within the basal plane, only phonons polarized along z can contribute to this process.

Four phonon modes of graphene at the K point with energies clustered around 150 meV have in-plane polarizations (see Fig. 1) [24,25]. The remaining two degenerate phonon modes at energy $E_0 = 67$ meV are polarized along z, and these are the relevant ones. At low temperatures, phonon absorption is quenched. Photoemission assisted by phonon emission should exhibit a gap of 67 meV below the Fermi level E_F by energy conservation. At finite temperatures, the photoemission intensity becomes

$$I(E) \propto (A - BE)\Big[F(E - E_F + E_0; T) + \exp\Big(\frac{-E_0}{k_B T}\Big)F(E - E_F - E_0; T)\Big], \tag{5}$$

where F is the Fermi-Dirac distribution function, and the factor $\exp(-E_0/k_BT)$ is the branching ratio between phonon absorption and emission processes. The effective (phonon-assisted) density of states and cross section variations are assumed to be linear (with A and B being constants). At high temperatures, phonon absorption processes could fill in the gap. However, with $E_0/k_B = 770$ K, the gap remains visible even at room temperature. The red (medium gray) curves [Fig. 2(d)] are fits to the data at temperatures $T = 60$ and 300 K using Eq. (5) supplemented by a metallic Fermi edge to simulate defect scattering. The fits yield $E_0 = 64$ meV, in good agreement with the known value of 67 meV. Analysis of the other cases [e.g., Fig. 2(e)] yields similar values of E_0 within a few meV.

A gap of similar size was reported in a scanning tunneling spectroscopy study of graphene [26,27], and it was attributed to phonon-mediated inelastic tunneling [28]. However, there have been disagreements about the gap size or even the existence of gaps [29–32]. The inconsistencies remain controversial and could be related to sample inhomogeneity, tip structure, or tunneling at the buried interface. The mechanism leading to the ARPES gap does not apply directly to the tunneling case. However, for a well collimated tunneling current perpendicular to the graphene layers from a tip with a simple density of states, the same parity selection rules apply, and a gap of ~67 meV can be expected.

ARPES is free from tip effects; a further advantage is angular resolution. Experimentally, the gap disappears for increasing emission angle or in-plane momentum [Fig. 4(a)]; the symmetrized spectra are for 3 ML graphene on SiC at 60 K. The two vertical lines indicate the edges of the gap at normal emission. The corresponding first derivatives [Fig. 4(b)] show peaks at the edges of the gap. The gap diminishes and gets filled in for increasing emission angles because phonons at lower wave vectors, and lower energies, become involved.

While the 67 meV phonons are the dominant contributions to the gap at normal emission, other phonons at ~150 meV are expected to contribute as well, however weakly. The dipole transition term, even though suppressed, is nonzero, and its parity permits the excitation of the in-plane phonons. High-resolution scans indeed

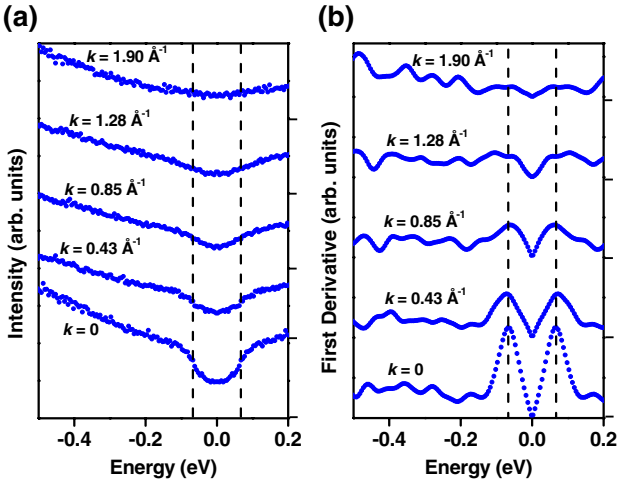

FIG. 4 (color online). Dependence of the gaps on **k**. (a) Symmetrized spectra for 3 ML graphene as a function of in-plane momentum **k** along the $\bar{\Gamma}\bar{K}$ direction. The photon energy used was 50 eV. (b) Absolute value of the first derivative of (a). The zero level for each spectrum is indicated by a tick mark on the right vertical axis.

show a very weak secondary gap at ~150 meV (see [18]). The results suggest the possibility of detailed phonon spectroscopy based on this method.

The present study demonstrates that ARPES spectral regions forbidden for direct emission provide a valuable test ground for detailed investigations of elementary interactions. Electron-phonon coupling is a weak interaction, but its signature shows up clearly because of the absence of other spectral features. This insight is important for a detailed understanding of the basic physics of graphite and graphene [33,34]. Possible applications of the method include phonon spectroscopy and determination of the electron-phonon coupling strength through a detailed analysis of ARPES data. Specifically, the phonon gaps at general points in the Brillouin zone could be used to extract detailed phonon dispersion relations, while the spectral height of each phonon gap provides a direct measure of the electron-phonon coupling strength.

This work is supported by the U.S. Air Force Office of Scientific Research (Grant No. FA9550-09-1-030B). The Synchrotron Radiation Center, where the ARPES work was performed, is supported by the U.S. National Science Foundation (Grant No. DMR-05-37588). We acknowledge the Petroleum Research Fund, administered by the American Chemical Society, and the U.S. National Science Foundation (Grant No. DMR-09-06444) for partial support of the beam line facilities and operations. The NSCG sample was obtained from Chanyong Hwang of the Korea Research Institute of Standards and Science.

*tcchiang@illinois.edu

[1] S. Hüfner, *Photoelectron Spectroscopy* (Springer-Verlag, New York, 1996), 2nd ed.
[2] S. Y. Zhou, G.-H. Gweon, and A. Lanzara, Ann. Phys. (N.Y.) **321**, 1730 (2006).
[3] A. Bostwick, T. Ohta, T. Seyller, K. Horn, and E. Rotenberg, Nature Phys. **3**, 36 (2007).
[4] A. Damascelli, Z. Hussain, and Z.-X. Shen, Rev. Mod. Phys. **75**, 473 (2003).
[5] G. Grimvall, *The Electron-Phonon Interaction in Metals* (North Holland, Amsterdam, 1981).
[6] B. A. McDougall, T. Balasubramanian, and E. Jensen, Phys. Rev. B **51**, 13 891 (1995).
[7] T. Ohta, A. Bostwick, Th. Seyller, K. Horn, and E. Rotenberg, Science **313**, 951 (2006).
[8] S. Y. Zhou *et al.*, Nature Mater. **6**, 770 (2007).
[9] T. Ohta *et al.*, Phys. Rev. Lett. **98**, 206802 (2007).
[10] A. H. Castro Neto, F. Guinea, N. M. R. Peres, K. S. Novoselov, and A. K. Geim, Rev. Mod. Phys. **81**, 109 (2009).
[11] X. Gonze *et al.*, Comput. Phys. Commun. **180**, 2582 (2009).
[12] X. Gonze *et al.*, Z. Kristallogr. **220**, 558 (2005).
[13] X. Gonze, Phys. Rev. B **55**, 10 337 (1997).
[14] X. Gonze and C. Lee, Phys. Rev. B **55**, 10 355 (1997).
[15] M. Lazzeri, C. Attaccalite, L. Wirtz, and F. Mauri, Phys. Rev. B **78**, 081406(R) (2008).
[16] A. Grüneis *et al.*, Phys. Rev. Lett. **100**, 037601 (2008).
[17] N. M. R. Peres, F. Guinea, and A. H. Castro Neto, Phys. Rev. B **73**, 125411 (2006).
[18] See supplementary material at http://link.aps.org/supplemental/10.1103/PhysRevLett.105.136804.
[19] G. Somorjai, *Chemistry in Two Dimensions: Surfaces* (Cornell University Press, Ithaca, 1981).
[20] K. V. Emtsev, F. Speck, Th. Seyller, L. Ley, and J. D. Riley, Phys. Rev. B **77**, 155303 (2008).
[21] H. J. Levinson, E. W. Plummer, and P. J. Feibelman, Phys. Rev. Lett. **43**, 952 (1979).
[22] T. Miller, W. E. McMahon, and T.-C. Chiang, Phys. Rev. Lett. **77**, 1167 (1996).
[23] J. Hermanson, Solid State Commun. **22**, 9 (1977).
[24] M. Mohr *et al.*, Phys. Rev. B **76**, 035439 (2007).
[25] A. Grüneis *et al.*, Phys. Rev. B **80**, 085423 (2009).
[26] V. W. Brar *et al.*, Appl. Phys. Lett. **91**, 122102 (2007).
[27] Y. Zhang *et al.*, Nature Phys. **4**, 627 (2008).
[28] T. O. Wehling, I. Grigorenko, A. I. Lichtenstein, and A. V. Balatsky, Phys. Rev. Lett. **101**, 216803 (2008).
[29] G. Li, A. Luican, and E. Y. Andrei, Phys. Rev. Lett. **102**, 176804 (2009).
[30] E. Sutter, D. P. Acharya, J. T. Sadowski, and P. Sutter, Appl. Phys. Lett. **94**, 133101 (2009).
[31] P. Lauffer *et al.*, Phys. Rev. B **77**, 155426 (2008).
[32] D. L. Miller *et al.*, Science **324**, 924 (2009).
[33] K. S. Novoselov *et al.*, Nature (London) **438**, 197 (2005).
[34] Y. Zhang, Y.-W. Tan, H. L. Stormer, and P. Kim, Nature (London) **438**, 201 (2005).